TECHNICAL MEMORANDUMS

NATIONAL ADVISORY COMMITTEE FOR AERONAUTICS

No. 950

BUCKLING TESTS WITH A SPAR-RIB GRILL

By Josef Weinhold

Washington
September 1940

NATIONAL ADVISORY COMMITTEE FOR AERONAUTICS

TECHNICAL MEMORANDUM NO. 950

BUCKLING TESTS WITH A SPAR-RIB GRILL*

By Josef Weinhold

SUMMARY

The present report deals with a comparison of mathe-
matically and experimentally defined buckling loads of
a spar-rib grill, on the assumption of constant spar sec-
tion, and infinitely closely spaced ribs with rigidity
symetrical to the grill center. The loads are applied
as equal bending moments at both spar ends, as compres-
sion in the line connecting the joints, and in the spar
center line as the assumedly uniformly distributed spar
weight. The evaluation formula is valid for a deflec-
tion following a half wave, and confirmed by the tests
within a scope sufficient for practical purposes. The
formula is applicable with safety in the ratio bounded by
by experiments between the end moments and the compres-
sive force, or between the coefficients s, m_1, and m_2,
respectively.

An effect of the finite aspect ratio of test spars
(8 : 100) is practically not noticeable. For smaller
compressive forces and greater end moments the coeffi-
cients of the evaluation formula should be computed again
for further deflection forms, in order to find further
buckling conditions, which, of course, yield lower loads
at the stability limit. For small spar weight a buckling
condition exact for vanishing weight, which is written
down for arbitrary wave number of the deflections, may be
employed for the first comparison, which wave number
gives the lowest buckling load. An extension of the en-
ergy equation and consequently the achievement of a buck-
ling condition for any degree of rib rigidity along the
rib axis and other load distribution is readily accom-
plished.

Notation

M_1, M_2*	bending moment in the spar ends, mkg
S_1, S_2	compressive force in line connecting the joints, kg
G_1, G_2	spar weight, acting in beam axis, kg
A_1, A_2	rigidity of transverse bending, kgm^2
C_1, C_2	torsional rigidity of spars, kgm^2
Ar	sum of rigidity of all ribs for buckling in the plane of the grill, kgm^2
Br	sum of rigidity of all ribs for buckling at right angle to plane of grill, kgm^2
A_{Ar}	strain energy of ribs for the spar length 1 by buckling in the plane of grill, kgm/m
B_{Br}	strain energy of ribs for the spar length 1 by buckling at right angle to plane of grill, kgm/m
κ_1, κ_2, κ_3	nondimensional free value
h	half distance of beam axes, m
l	distance of spar joints (spar length), m
m_1, m_2	end moments of a rib for spar length 1, kgm/m
n	half-wave number in the course of η, β_1, and β_2
c_1, c_2	numerical values of part integrals in the energy equation
x	longitudinal coordinate, counted from a joint, m
y	lateral deflection of beam axes at distance x from joint, m

---

*Subscripts 1 and 2 denote — if used alone — that the particular quantity belongs to spar 1 and spar 2, respectively. Without subscript the quantities apply to both spars unless stated otherwise.

β_1, β_2 buckling angle (angle of rotation of spar sections at right angle to plane of grill)

α_1, α_2 influence figures

$\xi = x/l$ nondimensional longitudinal coordinate

$\eta = y/l \sqrt{\dfrac{A_1 + A_2}{C_1 + C_2}}$ nondimensional lateral deflection

Nondimensional quantities in the energy equation:

$$m_1 = \frac{2 M_1 l}{\sqrt{(A_1 + A_2)(C_1 + C_2)}} \;, \qquad m_2 = \frac{2 M_2 l}{\sqrt{(A_1 + A_2)(C_1 + C_2)}}$$

$$s = \frac{(S_1 + S_2) l^2}{A_1 + A_2}$$

$$g_1 = \frac{G_1 l^2}{\sqrt{(A_1 + A_2)(C_1 + C_2)}} \;, \qquad g_2 = \frac{G_2 l^2}{\sqrt{(A_1 + A_2)(C_1 + C_2)}}$$

$$a = \frac{2 Ar l}{(A_1 + A_2)h} \;, \qquad b = \frac{2 Br l}{(C_1 + C_2)h}$$

$$\mu_1 = \frac{2 C_1}{C_1 + C_2} \;, \qquad \mu_2 = \frac{2 C_2}{C_1 + C_2}$$

$$\zeta_1 = \frac{\alpha_1}{\alpha_1^2 - \alpha_2^2} \;, \qquad \zeta_2 = \frac{\alpha_2}{\alpha_1^2 - \alpha_2^2} \;, \qquad \zeta_3 = \frac{1}{\alpha_3 - \alpha_4}$$

INTRODUCTION

Earlier reports give buckling loads which were derived under specified simplifying premises and assumptions (references 1 and 2). In particular, the spars were assumed as small rails with vanishing thickness and equal constant section for both spars. It is further assumed that the rib rigidity is constant and uniformly distributable across the length of the spar. (Infinitely closely

spaced ribs as substitute of finite number of ribs.) End
bending moments and end compressive forces were assumed
as spar loads.

The following describes an investigation which enables
a comparison of computed and experimentally defined buck-
ling loads of a spar-rib grill. The experimental grill
has dissimilar spars which are not "very small" (8/100 mm),
the number of ribs, 8, is comparatively low). The rigid-
ity of the ribs is no longer constant across the axis,
although not symmetrically distributed with respect to the
rib center. In the evaluation formula, which ordinarily
is derived under the same general assumptions from the
energy equation as before (reference 2), the dissimilarity
of the spars, the cited course of rib rigidity, and the
spar weight are allowed for.

Experimental Arrangement*

The spars of the model grill are two pine boards
8 by 100 by 3250 mm, selected for grain, absence of knots,
etc., and the ribs (7 by 7 by 1000 mm) of the same grade
of pine with reinforcement strips glued at the ends (fig.
2). Spar and rib end are fastened together by a 12-by-12-
by-0.5-mm hard drawn brass angle and five 3-mm bolts. The
spacing of the spar axes from each other amounts to 2h =
1025 mm. A hardened steel cylinder drilled out with a
taper from each side and fitting tightly in the spar end
reinforced by plywood shims, serves as nodal point of the
spar ends. The annular edge within the cylinder has an
8-mm diameter and rests against a hardened round steel bar
of 7-mm diameter. This in turn is fastened on one grill
end to the support, on the other spar end the slidability,
shown in figures 1 and 2, parallel with the line connect-
ing the nodal points, is provided. The end moments are
transmitted over fixed end levers built up of 10-by-1-mm
flat brass and 10-by-10-by-1-mm angle brass, which project
to 560-mm load application. For applying the axial com-
pression, the fixed joint near the spars carries two ball-
bearing pulleys over which the tension of the loading
weights is carried parallel with the connecting line of
the joints to the movable joint. Wooden bars with metal
sting fitted at the end levers of spar 2 record the tan-
gential inclination of the elastic line in the joints, on
a little board with a sheet of paper. The length of the
tracing levers from joint to metal sting is 1020 mm. The
end moment existing on spar 1 as a result of the weight of

---

*See fig. 1.

the end levers and of the overhanging spar portion is
0.082 mkg, and 0.100 mkg on spar 2 because of the trac-
ing levers. The effective weight on the joints (weight
of spars plus weight of ribs) is equalized for each spar
at 1.21 kg. The buckling angles in joints are preserved
by 1-m wooden levers running parallel upward from the spar
ends with a loose pin or stud at the end parallel to the
connecting line of the joints. The guide is adjustable
perpendicularly to the line connecting the joints. Fig-
ure 4 shows the first set-up, where the spar plus the
rib weight was upwardly compensated by pulleys. But this
compensation had to be abandoned in favor of a more com-
plicated evaluation formula because the oscillations of
the grill could not be removed quickly enough after load
changes. Neither figure 4 nor figure 3 represents the
final method.*

<center>Evaluation Formula</center>

The energy equation for elastically identical spars
with a load through M_1, M_2 and S_1 and S_2 and ribs
of constant section (reference 2) reads:

$$J = \int_0^l \left\{ (M_1\beta_1 + M_2\beta_2)y'' - \left(\frac{S_1 + S_2}{2} - 3\frac{Ar}{lh} \right)y'^2 \right.$$

$$\left. + \frac{Br}{lh}(\beta_1^2 + \beta_1\beta_2 + \beta_2^2) + \frac{1}{2}C(\beta_1'^2 + \beta_2'^2) + A y''^2 \right\}dx \tag{1}$$

or in nondimensional coordinates and coefficients

$$\underline{F} = \int_0^1 \left\{ \underline{m}_1\beta_1 + \underline{m}_2\beta_2) \eta'' - (\underline{s} - 3\underline{a})\eta'^2 + \underline{b}(\beta_1^2 + \beta_1\beta_2 + \beta_2)^2 \right.$$

$$\left. + \frac{1}{2}(\beta_1'^2 + \beta_2'^2) + \eta''^2 \right\}d\xi \tag{2}$$

M_1 and M_2 are the principal moments bending at point x.

---

*The tests were made in the German Technical Institute at
Brünn, but had to be interrupted during the general mobil-
ization in September 1938. The means for the tests had
been furnished by the National Research Council of Czecho-
slovakia.

Accordingly, by virtue of the annexed loading schedule, M_1 and M_2 must be replaced by, respectively,

$$M_1 - \frac{G_1}{2l}(xl - x^2) \quad \text{and} \quad M_2 - \frac{G_2}{2l}(xl - x^2)$$

For the derivation of the proportions with Ar and Br the buckling of a rib at right angle to the plane of the grill due to the reaction parts transmitted at the joints, is expressed conformally to figure 7, with

$$\beta_1 = \frac{hl}{Br}(m_1 \alpha_1 - m_2\alpha_2), \qquad \beta_2 = \frac{hl}{Br}(m_2\alpha_1 - m_1 \alpha_2) \qquad (3)$$

(The rib rigidity is $\frac{Br}{l}$, the rigidity for spar length l.)

Then the energy content of the rib is

$$A_{Br} = \frac{Br}{2 h l(\alpha_1{}^2 - \alpha_2{}^2)}(\alpha_1(\beta_1{}^2 + \beta_2{}^2) + 2 \alpha_2\beta_1\beta_2) \qquad (4)$$

For buckling in the plane of the grill, it affords in the same way

$$A_{Ar} = \frac{Ar}{h l(\alpha_3 - \alpha_4)} y'^2 \qquad (5)$$

if y' (reference 2) replaces β_1 and β_2, and α_3 and α_4 replace α_1 and α_2.

The sum then is

$$J = \int_0^l \left[\left\{ \left(M_1 - \frac{G_1}{2l}(xl - x^2) \right) \beta_1 + \left(M_2 - \frac{G_2}{2l}(xl - x^2) \right) \beta_2 \right\} y'' \right.$$

$$- \left(\frac{S_1 + S_2}{2} - \frac{Ar}{hl(\alpha_3 - \alpha_4)} \right) y'^2 + \frac{Br(\alpha_1(\beta_1{}^2 + \beta_2{}^2) + 2\alpha_2\beta_1\beta_2}{2 h l(\alpha_1{}^2 - \alpha_2{}^2)}$$

$$\left. + \frac{1}{2} C_1\beta_1'^2 + \frac{1}{2} C_2\beta_2'^2 + \frac{1}{2} (A_1 + A_2)y''^2 \right] d x \qquad (6)$$

Extension with $\frac{2l^2}{C_1 + C_2}$, followed by introduction of the nondimensional coordinates and abbreviations, gives:

$$\underline{F} = \int_0^1 \left[\left\{ (\underline{m}_1 - \underline{g}_1(\xi - \xi^2))\beta_1 + (\underline{m}_2 - \underline{g}_2(\xi - \xi^2))\,\beta^2 \right\} \eta'' \right.$$

$$- (\underline{s} - \zeta_3\,\underline{a})\eta'^2 + \frac{1}{2}\,\underline{b}\,(\zeta_1(\beta_1{}^2 + \beta_2{}^2) + 2\,\zeta_2\,\beta_1\beta_2)$$

$$\left. + \frac{1}{2}\,\mu_1\beta_1'^2 + \frac{1}{2}\,\mu_2\beta_2'^2 + \eta''^2 \right] d\,\xi \tag{7}$$

The limiting conditions adapted to the described test arrangement read (case 1, reference 2):

$$\left. \begin{array}{c} \eta(0) = \eta(1) = \eta''(0) = \eta''(1) = 0 \\[2mm] \beta_1(0) = \beta_1(1) = \beta_2(0) = \beta_2(1) = 0 \end{array} \right\} \tag{8}$$

These are experimentally much easier to keep than others and give at the same time lower buckling loads in ratio to built-in spars.

The related differential equations following from the disappearance of the first variation of equation (7) are:

$$\frac{1}{2}\,\frac{d^2}{d\,\xi^2}\left\{ (\underline{m}_1 - \underline{g}_1(\xi - \xi^2))\beta_1 + (\underline{m}_2 - \underline{g}_2(\xi - \xi^2))\,\beta_2 \right\}$$

$$+ \eta^{IV} + (\underline{s} - \zeta_3\underline{a})\eta'' = 0 \tag{9}$$

$$\left. \begin{array}{c} (\underline{m}_1 - \underline{g}_1(\xi - \xi^2))\eta'' - \mu_1\beta_1'' + \underline{b}(\zeta_1\beta_1 + \zeta_2\beta_2) = 0 \\[2mm] (\underline{m}_2 - \underline{g}_2((\xi - \xi^2))\eta'' - \mu_2\beta_2'' + \underline{b}(\zeta_2\beta_1 + \zeta_1\beta_2) = 0 \end{array} \right\} \tag{10}$$

After two integrations of equation (9) the integration constants disappear as a result of the chosen limiting conditions, leaving the simpler relation

$$\frac{1}{2}\,(\underline{m}_1 - \underline{g}_1(\xi - \xi^2))\beta_1 + \frac{1}{2}(\underline{m}_2 - \underline{g}_2(\xi - \xi^2))\,\beta_2$$

$$+ \eta'' + (\underline{s} - \zeta_3\underline{a})\eta = 0 \tag{9a}$$

For vanishing spar weight equations (9) and (10) are satisfied by

$$B_1 = \kappa_1\sin n\,\pi\,\xi, \quad \beta_2 = \kappa_2\sin n\,\pi\,\xi, \quad \eta = \kappa_3\sin n\,\pi\,\xi \tag{11}$$

The final determinant remaining after the insertion of the solutions (11) gives the buckling condition

$$\frac{1}{2}\frac{m_1^2}{(n\pi)^2}(\mu_2(n\pi)^2 + \zeta_1 \underline{b}) + \frac{1}{2}\frac{m_2^2}{(n\pi)^2}(\mu_1(n\pi)^2 + \zeta_1 \underline{b})$$

$$-\frac{m_1 m_2}{(n\pi)^2}\zeta_2\underline{b} + \left(\frac{s - \zeta_3\underline{a}}{(n\pi)^2} - 1\right)$$

$$\left\{\mu_1\mu_2(n\pi)^2 + 2\zeta_1\underline{b} + (\zeta_1^2 - \zeta_2^2)\underline{b}^2/(n\pi)^2\right\} = 0 \qquad (12)$$

The exact solution of the complete differential equations was foregone for reasons of the paper work involved, and the evaluation formula therefore derived by presentation of suitably chosen approximating theorems in the energy equation. Chosen as such were:

$$\text{I. } \beta_1 = \frac{1}{\kappa_1}(\xi - \xi^2), \ \beta_2 = \frac{1}{\kappa_2}(\xi - \xi^2), \ \eta'' = \frac{1}{\kappa_3}(\xi - \xi^2) \qquad (13)$$

$$\text{II. } \beta_1 = \frac{1}{\kappa_1}(\xi - 2\xi^3 + \xi^4), \ \beta_2 = \frac{1}{\kappa_2}(\xi - 2\xi^3 + \xi^4), \ \eta'' = \frac{1}{\kappa_3}(\xi - 2\xi^3 + \xi^4) \qquad (14)$$

In order to clarify the mutual relations of the coefficients in the buckling equation the numerical values of the part integrals in the energy equation are generalized:

$$\frac{1}{\kappa_1^2}\int_0^1 \beta_1^2 \, d\xi = \frac{1}{\kappa_2^2}\int_0^1 \beta_2^2 \, d\xi = \frac{1}{\kappa_1\kappa_2}\int_0^1 \beta_1\beta_2 \, d\xi$$

$$= \frac{1}{\kappa_3^2}\int_0^1 \eta''^2 d\xi = \frac{1}{\kappa_1\kappa_3}\int_0^1 \beta_1\eta'' \, d\xi = \frac{1}{\kappa_2\kappa_3}\int_0^1 \beta_2\eta'' d\xi = c_1 \qquad (15)$$

$$\frac{1}{\kappa_1^2}\int_0^1 \beta_1'^2 \, d\xi = \frac{1}{\kappa_2^2}\int_0^1 \beta_2'^2 \, d\xi = c_2 \qquad (16)$$

$$\frac{1}{\kappa_3^2}\int_0^1 \eta'^2 \, d\xi = c_3 \qquad (17)$$

$$\frac{1}{\kappa_1 \kappa_3} \int_0^1 \eta'' \beta_1 (\xi - \xi^2) \, d\xi = \frac{1}{\kappa_2 \kappa_3} \int_0^1 \eta'' \beta_2 (\xi - \xi^2) \, d\xi = c_4 \quad (18)$$

With these data the energy equation (7) supplies as buckling condition

$$\left. \begin{aligned}
&\frac{1}{2} \left(\mu_2 \frac{c_2}{c_1} + \zeta_1 \underline{b} \right) \left[\frac{c_1}{c_2} m_1^{\,2} - 2 \frac{c_4}{c_2} \underline{m}_1 \underline{g}_1 + \underline{g}_1^{\,2} \frac{c_4^{\,2}}{c_1 c_2} \right] \\[2mm]
&+ \frac{1}{2} \left(\mu_1 \frac{c_2}{c_1} + \zeta_1 \underline{b} \right) \left[\frac{c_1}{c_2} \underline{m}_2^{\,2} - 2 \frac{c_4}{c_2} \underline{m}_1 \underline{g}_1 + \underline{g}_2^{\,2} \frac{c_4^{\,2}}{c_1 c_2} \right] \\[2mm]
&- \underline{b} \; \zeta_2 \left[\frac{c_1}{c_2} \underline{m}_1 \underline{m}_2 - \frac{c_4}{c_2} (\underline{m}_1 \underline{g}_1 + \underline{m}_2 \underline{g}_2) + \underline{g}_1 \underline{g}_2 \frac{c_4^{\,2}}{c_1 c_2} \right] \\[2mm]
&+ \frac{c_3}{c_1} (\underline{s} - \zeta_3 \underline{a}) - 1 \Big) \left\{ \mu_1 \mu_2 \frac{c_2}{c_1} + 2 \zeta_1 \underline{b} + (\zeta_1^{\,2} - \zeta_2^{\,2}) \underline{b}^2 \frac{c_1}{c_2} \right\} = 0
\end{aligned} \right\} \quad (19)$$

The numerical values of c_1, c_2 . . . and their combinations are given for approximations I and II in the second and third lines of table I.

A comparison of equation (19) with the exact solution (12) discloses, then, $\frac{c_2}{c_1}$ and $\frac{c_1}{c_3}$ for π^2. Moreover, the limiting conditions considered here give for Timoshenko's (reference 3) exact buckling factor

$$G \; l^2 \Big/ \sqrt{A \, C} = 28.3 \quad (20)$$

for $\frac{c_1 c_2}{c_4^{\,2}}$ the actual value $\frac{1}{4}\, 28.3^2 = 200.22_3$. The third approximation and final evaluation formula employed is that in which $\frac{c_2}{c_1}$, $\frac{c_1}{c_3}$, and $\frac{c_1 c_2}{c_4^{\,2}}$ are replaced by the exact values and $\frac{c_2}{c_4}$ by the value 44.4535, the latter following from $\frac{c_2}{c_1} = \pi^2$ and $\frac{c_1 c_2}{c_4^{\,2}} = 200.22_3$ and which probably differs very little and nonessentially from the true value

$$\frac{1}{2}\left(\mu_2\pi^2 + \zeta_1\underline{b}\right)\left[\frac{m_1{}^2}{\pi^2} - \frac{m_1\,g_1}{22.23} + \frac{g_1{}^2}{200.22}\right]$$

$$+ \frac{1}{2}\left(\mu_1\pi^2 + \zeta_1\underline{b}\right)\left[\frac{m_2{}^2}{\pi^2} - \frac{m_2\,g_2}{22.23} + \frac{g_2{}^2}{200.22}\right]$$

$$- \zeta_2\underline{b}\left[\frac{m_1m_2}{\pi^2} - \frac{m_1g_1 + m_2g_2}{44.45} + \frac{g_1\,g_2}{200.22}\right]$$

$$+ \left(\frac{s - \zeta_3\underline{a}}{\pi^2} - 1\right)\left\{\mu_1\mu_2\pi^2 + 2\zeta_1 b + \left(\zeta_1{}^2 - \zeta_2{}^2\right)\frac{b^2}{\pi^2}\right\} = 0 \qquad (21)$$

A_1, C_1, A_2, C_2 were defined from buckling tests with one single spar each without ribs attached. The related evaluation formula follows from the above after insertion of $M_1 = M_2 = M$, $S_1 = S_2 = S$, $\underline{a} = 0$, $b = 0$, and the expressions for $\underline{s}$, $\underline{m}_1$, and $\underline{m}_2$ in the form

$$\frac{M^2\,l^2}{\pi^2} - \frac{G\,l^2\,M\,l}{44.45} + \frac{G^2\,l^4}{800.89} + \frac{C\,S\,l^2}{\pi^2} = A\,C \qquad (22)$$

Test Procedure

The first tests were made without the weights suspended from the end lever, one horizontal pull cord being used to transmit the principal part of the load, and then the other. After various attempts the locations of the cylinders slipped in the spar ends were finally established for which the deflections by equal load near the stability limit were lowest. The inclination of the elastic line at the spar ends served, as already indicated, as deflection component, the board with the sheet of paper being pressed against the tracing lever after the set-up ceases to swing and the load is written alongside the tracing mark. The adjusting levers for end-buckling angle remained loosely in the guides. For further tests with this setting the grill was fitted with 7 kg end-lever loads on spar 1, on spars 1 and 2, and then on spar 2. The applied load at the end levers could be shifted transversely to the beam axis, and so far that after application of the end-lever load the resetting lever over the joints was loose again in the guides. Thus the end load was applied in consistently smaller stages till the lateral deflection in

spar center reached about 100 mm. Greater deflections
produced appreciable permanent deformations. Up to 100
mm lateral deflection in spar center the permanent de-
flection, after applied end load, was at the most 1.5 mm
at the pointer tip. For the same reasons the recording
of a supercritical branch of the stress-strain diagram,
as by Prandtl (reference 4) was omitted. The height of
the critical end load had to be determined, therefore,
as hyperbolic asymptote height by known asymptote direc-
tions and three given hyperbola points (reference 5).
The force deflection diagrams taken at both ends of spar
2 differ very little, which is indicative of the symmet-
rical course of the deflections. Tests with 10-kg end-
lever load left perceptible permanent deformations, es-
pecially in the spar-rib connections and the symmetrical
course of the deflections disappeared. The evaluation
formula would then give too high comparative values. Ex-
periments and comparisons in this direction with an im-
proved set-up are under way.

Table II contains the end moments M_1, M_2 applied
at the grill, and the related end compressive forces de-
termined from the deflection plots. Figure 8 is the dia-
gram showing the comparatively greater departure from the
presumed symmetry of deflection, whose equilibrium curves
have the relatively greater distance from the asymptotes.
$S_1 + S_2 = 11.26$ kg is the sum of the "scale loading" of
10.8 kg determined by the asymptote construction and the
"scale weight" of 0.457 kg identical for all the tests.

Spar Rigidity A_1, C_1, A_2, C_2

Following the buckling tests with the model grill
the ribs were removed and each spar tested at three dif-
ferent end moments. The effective weight of each spar was
0.980 kg. The three load systems are appended in table
III. Equation (22) gives for A_1, C_1, A_2, C_2 three equa-
tions each which, interconnected, give each three pairs
of rigidity A and C. Their averages

$A_1 = 4.961$ m²kg $C_1 = 0.605$ m²kg

$A_2 = 4.978$ m²kg $C_2 = 0.633$ m²kg

served as a basis in the subsequent calculations.

Determination of Rigidity Factors $\zeta_1\underline{b}$, $\zeta_2\underline{b}$, and $\zeta_3\underline{a}$

Two each of the eight ribs spaced 15 cm apart were attached to a 20-cm long piece of spar in the same way as on the grill and supported and loaded. The torsion angles over the joints were determined by means of mirror reading and compiled in table IV. It shows the extent to which the symmetry assumption is satisfied for the course of rib rigidity along the rib axis. Equation (3) and the equations defining b, ζ_1, and ζ_2 give

$$\underline{b}\zeta_1 = \frac{2\ m_1\ l^2\beta_1}{(C_1 + C_2)(\beta_1{}^2 - \beta_2{}^2)} \quad \text{and} \quad \underline{b}\zeta_2 = \frac{2\ m_1\ l^2\beta_2}{(C_1 + C_2)(\beta_1{}^2 - \beta_2{}^2)} \quad (23)$$

and in our case for the mean values of β_1, $\overline{\beta}_2$, and β_2, $\overline{\beta}_1$:

$$\zeta_1\underline{b} = 50.6, \quad \zeta_2\underline{b} = 26.5$$

$$\frac{1}{2}\left|\beta_1\right| + \frac{1}{2}\left|\overline{\beta}_2\right| = 0.0423, \quad \frac{1}{2}\left|\beta_2\right| + \frac{1}{2}\left|\overline{\beta}_1\right| = 0.0218$$

Test 4 without end-lever load affords $\zeta_3\underline{a}$, which gives $S_1 + S_2 = 16.52$ kg. The evaluation formula (21) then gives

$$\zeta_3\underline{a} = 5.14$$

According to the definition of $\zeta_3\underline{a}$, $\zeta_1\underline{b}$ and $\zeta_2\underline{b}$ should be – equal rigidity of ribs and their attachments in and at right angles to the plane of the grid being assumed –

$$\zeta_3\underline{a} = (\zeta_1 + \zeta_2)\underline{b}\ \frac{C_1 + C_2}{A_1 + A_2} = 77.1\ \frac{1.238}{9.949} = 9.6$$

The much lower actual value of 5.14 is due to the fact that the rib fittings are much more elastic with respect to buckling in the plane of the grill than at right angles to the plane of the grill. It might be noted in passing that the eight ribs had been selected from about 80 others. The sequence of arrangement on the spar is that of table IV, hence the pair closest to the average value is situated at spar center where the greatest twist occurred.

Comparison of Theoretical and Experimental Values

Table II gives the end moments, the critical compressive forces found from the force-deflection diagrams, the mathematical compressive forces, and the difference between the compressive forces in percent. In view of the uncertainty affecting the determination of the critical compression forces from force-deflection diagrams and particularly because of the dissimilarity of the ribs, the accord between theory and test may be termed satisfactory. Since the evaluation formula for the small rail is exactly valid, the critical experimental compressive forces should, on the whole, exceed the theoretical, which is the case in test 1 only. For the present 8:100 aspect ratio a pure moment loading through M_1 and M_2 with and without allowance for finite aspect ratio would give a difference of about 1 percent, which, however, is covered by the uncertainty of the coordination. In test 3 the difference between the theoretical and the experimental critical compressive force with -6.2 percent is greatest compared with the two previous tests. This can be associated with the previously stressed maximum departure from the symmetry hypothesis for the deformation and this in turn with the dissimilarity of the ribs.

Translation by J. Vanier,
National Advisory Committee
for Aeronautics.

REFERENCES

1. Weinhold, J.: Über die Kippstabilität von Holm-
     Rippenrosten. Z.f.a.M.M., vol. 17, no. 5, Oct.
     1937, pp. 270-275.

2. Weinhold, J.: Über die Kippstabilität der Holme im
     Rippenverband. Z.f.a.M.M., vol. 18, no. 5, Oct.
     1938, pp. 272-284.

3. Timoshenko, S.: Theory of Elastic Stability. McGraw-
     Hill Book Co., Inc. (New York), 1930.

4. Prandtl, L.: Kipperscheinungen. Inaugural-Diss.
     München 1899.

5. von Kármán, Th.: Untersuchungen über Knickfestigkeit.
     Mitt. über Forschungsarbeiten auf dem Gebiete des
     Ingenieurwesens, Heft 81.

TABLE I

Approx-imation	c_1	c_2	c_3	c_4	$\dfrac{c_2}{c_1}$	$\dfrac{c_2}{c_4}$	$\dfrac{c_1\,c_2}{c_4{}^2}$	$\dfrac{c_1}{c_3}$
I	$\dfrac{1}{30}$	$\dfrac{1}{3}$	$\dfrac{17}{35\times144}$	$\dfrac{1}{140}$	10	46.6	217.7	9.88235..
II	$\dfrac{31}{18\times35}$	$\dfrac{17}{35}$	$\dfrac{691}{99\times1400}$	$\dfrac{37}{3465}$	9.870968..	45.486..	209.607..	9.86975..
III	--	--	--	--	π^2	44.4535	200.223	π^2

TABLE II

Critical Outside Loads of Grill

Test	M_1 (mkg)	M_2 (mkg)	$(S_1+S_2)_{test}$ (kg)	$(S_1+S_2)_{theory}$ (kg)	F* (percent)
1	0.082	4.02	12.29	11.95	2.8
2	4.002	4.02	11.56	11.82	-2.2
3	4.002	.10	11.26	12.01	-6.2
4	.082	.10	16.52	16.52	-

*Difference between experimental and theoretical value in
  percent of computed value.

TABLE III

Buckling Loads for the Free Spars

Spar 1		Spar 2	
M (mkg)	S (kg)	M (mkg)	S (kg)
0.10	5.35	0.10	5.38
1.21	4.14	1.21	4.22
1.78	1.95	1.78	2.115

TABLE IV

Rib Torsion Angle for $m_1 \frac{1}{4}$ and $m_2 \frac{1}{4} = 0.0813$ mkg

Rib	β_1	β_2	$\overline{\beta}_1$	$\overline{\beta}_2$
1 2	0.0435	-0.0225	0.0228	-0.0438
3 4	.0431	- .0222	.0218	- .0427
5 6	.0419	- .0214	.0215	- .0416
7 8	.0409	- .0212	.0210	- .0409
Average	.04235	- .021825	.021775	- .04225
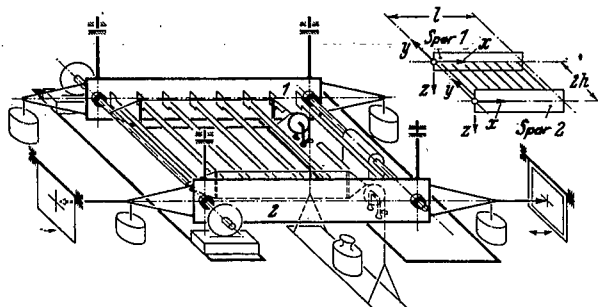
Figure 1.- Experimental set up.
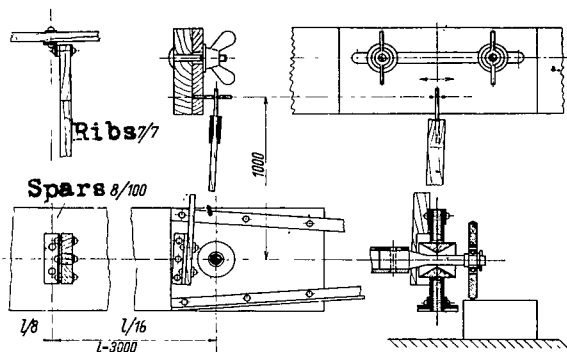
Figure 2.- Spar support, rib fitting and
adjustment of end buckling angle.
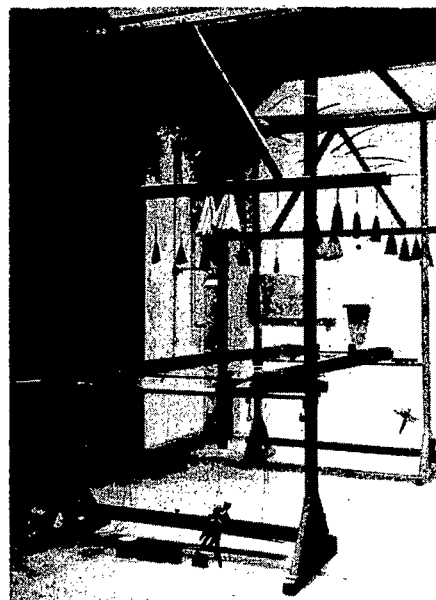
Figure 4.- First experimental
set up.
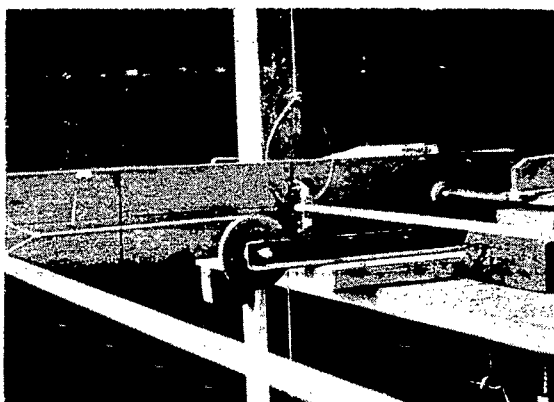
Figure 3.- Pulley at fixed joint.
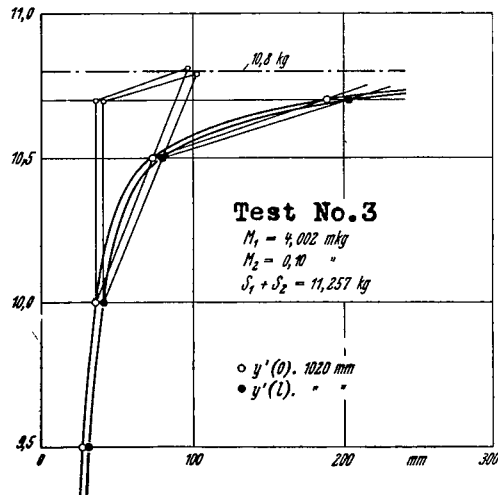
Figure 8.- Load-deflection
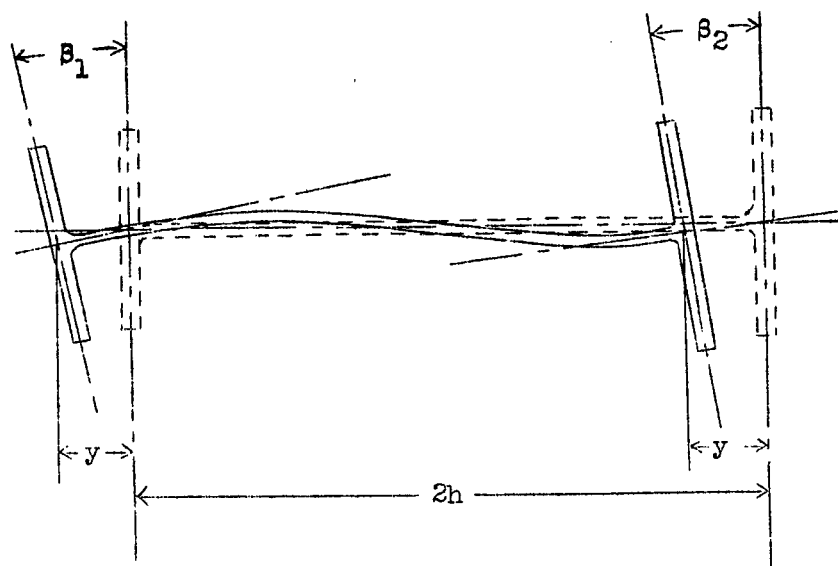diagram for test
No. 3.
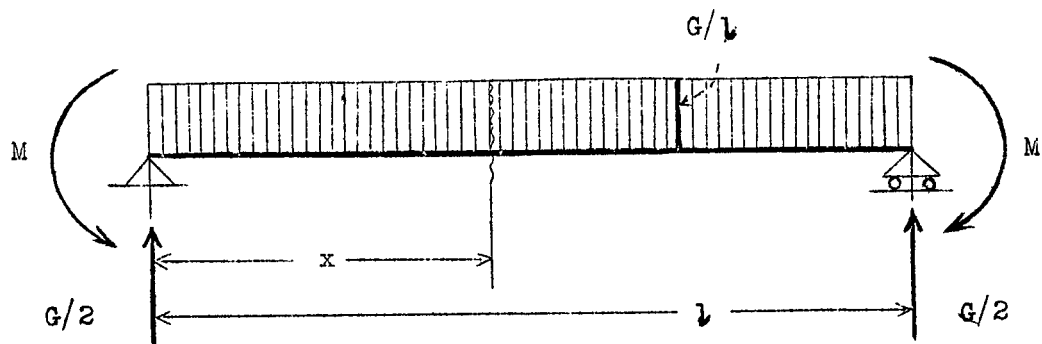
Figure 5.- Section at distance x from joint.

Figure 6.- Spar-bending loads.

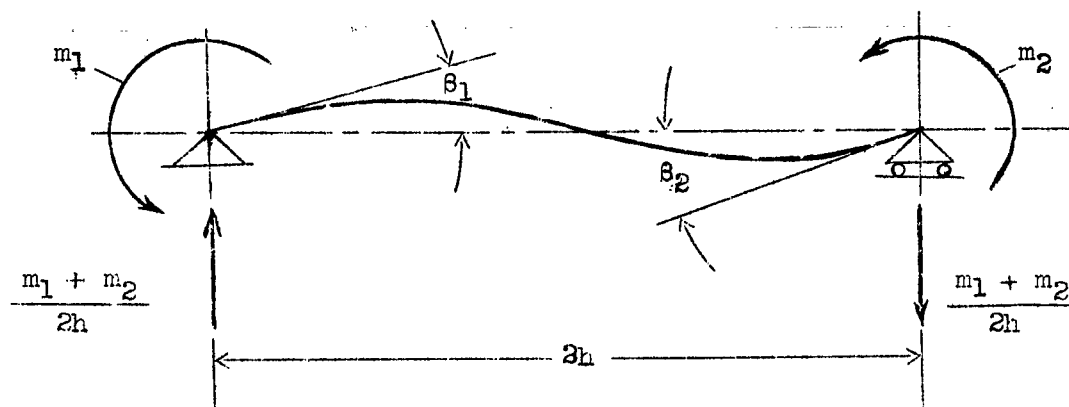Figure 7.- Strain of ribs due to bending at right angle
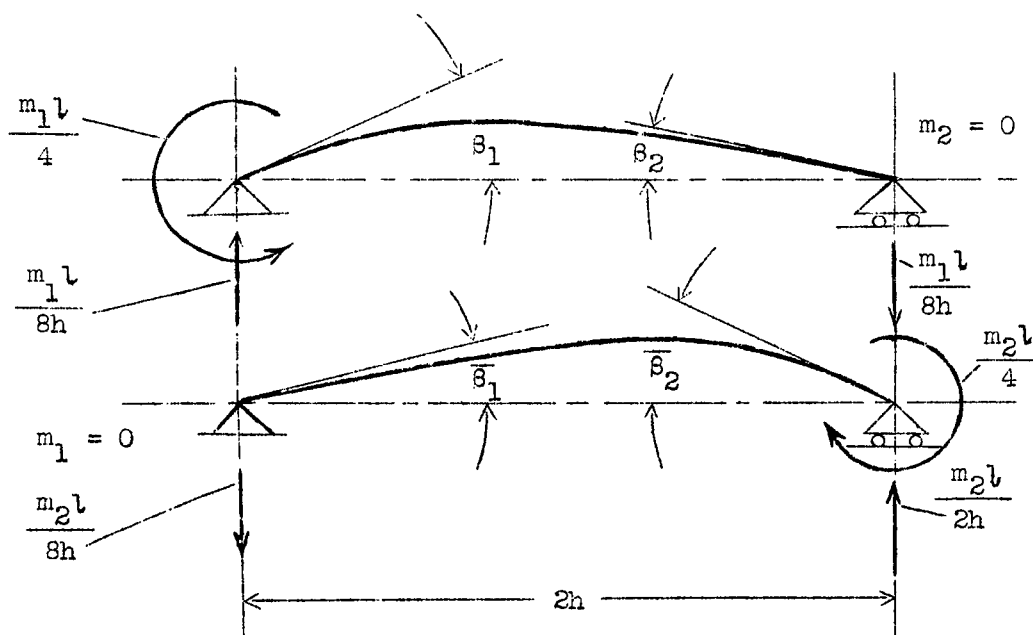to plane of grill.

Figure 9.- Test rigging for determining B_r.